JASN

J Am Soc Nephrol. 2017 Jun; 28(6): 1741–1752.
Published online 2017 Jan 6.
doi: 10.1681/ASN.2016020200: 10.1681/ASN.2016020200

PMCID: PMC5461783
PMID: 28062569

Inhibition of *αvβ5* Integrin Attenuates Vascular Permeability and Protects against Renal Ischemia-Reperfusion Injury

Amy McCurley,[*] Stella Alimperti,[†‡] Silvia B. Campos-Bilderback,[§] Ruben M. Sandoval,[§] Jenna E. Calvino,[*] Taylor L. Reynolds,[*] Catherine Quigley,[*] Joshua W. Mugford,[*] William J. Polacheck,[†‡] Ivan G. Gomez,[*] Jennifer Dovey,[*] Graham Marsh,[*] Angela Huang,[*] Fang Qian,[*] Paul H. Weinreb,[*] Brian M. Dolinski,[*] Shaun Moore,[*] Jeremy S. Duffield,[*] Christopher S. Chen,[†‡] Bruce A. Molitoris,[§‖] Shelia M. Violette,[*] and Michael A. Crackower[*]

[*]Biogen Inc., Cambridge, Massachusetts;
[†]Department of Biomedical Engineering, Boston University, Boston, Massachusetts;
[‡]The Wyss Institute for Biologically Inspired Engineering at Harvard University, Boston, Massachusetts;
[§]Indiana University School of Medicine, The Roudebush Veterans Affair Medical Center, Indiana Center for Biological Microscopy, Indianapolis, Indiana; and
[‖]Department of Cellular and Integrative Physiology, Indiana University School of Medicine, Indianapolis, Indiana
[✉]Corresponding author.
Correspondence: Dr. Amy Theresa McCurley, Biogen Inc., 225 Binney Street, Cambridge, MA 02142. Email: amy.mccurley@biogen.com
Present address: Dr. Michael A. Crackower, Celgene Corporation, Cambridge, Massachusetts.

Received 2016 Feb 18; Accepted 2016 Nov 22.

Abstract

Ischemia-reperfusion injury (IRI) is a leading cause of AKI. This common clinical complication lacks effective therapies and can lead to the development of CKD. The *αvβ5* integrin may have an important role in acute injury, including septic shock and acute lung injury. To examine its function in AKI, we utilized a specific function-blocking antibody to inhibit *αvβ5* in a rat model of renal IRI. Pretreatment with this anti-*αvβ5* antibody significantly reduced serum creatinine levels, diminished renal damage detected by histopathologic evaluation, and decreased levels of injury biomarkers. Notably, therapeutic treatment with the *αvβ5* antibody 8 hours after IRI also provided protection from injury. Global gene expression profiling of post-ischemic kidneys showed that *αvβ5* inhibition affected established injury markers and induced pathway alterations previously shown to be protective. Intravital imaging of post-ischemic kidneys revealed reduced vascular leak with *αvβ5* antibody treatment. Immunostaining for *αvβ5* in the kidney detected evident expression in perivascular cells, with negligible expression in the endothelium. Studies in a three-dimensional microfluidics system identified a pericyte-dependent role for *αvβ5* in modulating vascular leak. Additional studies showed *αvβ5* functions in the adhesion and migration of kidney pericytes *in vitro*. Initial studies monitoring renal blood flow after IRI did not find significant effects with *αvβ5* inhibition; however, future studies should explore the contribution of vasomotor effects. These studies identify a role for *αvβ5* in modulating injury-induced renal vascular leak, possibly through effects on pericyte adhesion and migration, and reveal *αvβ5* inhibition as a promising therapeutic strategy for AKI.

Keywords: acute renal failure, adhesion molecule, vascular, renal ischemia

Ischemia-reperfusion injury (IRI) after surgical procedures is a common in-hospital event that can result in AKI.[1] Originally thought to be a transient decrease in glomerular function, it is now clear that AKI frequently does not fully resolve and can contribute to the progression of CKD.[2] As a result there is a high rate of morbidity and mortality attributable to AKI.[3] Currently there is no pharmacologic therapy specifically approved for AKI after IRI.

Renal tubular injury is a key pathophysiologic outcome of IRI, however, it is known that AKI is a complex disorder resulting from inflammation and microvascular changes in addition to tubular injury.[4] Alterations in microvascular function, such as abnormal coagulation, increased vascular tone, and increased vascular permeability, promote inflammatory responses leading to continued ischemic conditions and further tissue injury.[5] Increased microvascular permeability is thought to result from loss of the integrity of the endothelium because of changes in the actin cytoskeleton and endothelial cell contacts.[6] Pericytes are also critical to the maintenance of microvascular barrier integrity.[7] Mice lacking pericytes have increased vascular permeability and the presence of pericytes has been shown to regulate permeability signaling and suppress inflammation, leading to enhanced barrier function.[7] After acute injury, renal pericytes have been shown to develop into myofibroblasts, contributing to the progression of CKD after AKI.[8] However, there are no data directly implicating kidney pericytes in vascular leak associated with AKI.

Integrins comprise a large family of membrane receptors that bind extracellular matrix proteins as well as other secreted proteins and membrane-tethered ligands. The RGD integrins are one class of integrins that bind this motif (arginine-glycine-aspartic acid), found in several extracellular matrix proteins. Integrin $\alpha v\beta 5$ is an RGD-binding integrin that binds to several extracellular ligands, including vitronectin[9] and milk fat globule protein E8 (MFG-E8).[10] $\alpha v\beta 5$ has been reported to be expressed in multiple cell types *in vitro*, including endothelial cells, epithelial cells, fibroblasts, and various leukocyte lineages.[11–15] A number of biologic functions have been attributed to $\alpha v\beta 5$, ranging from tumor angiogenesis[16] and phagocytosis[17] to adenoviral uptake,[18] fatty acid uptake,[19] and retinal pigment epithelium homeostasis.[20]

Several studies have also demonstrated a role of $\alpha v\beta 5$ in regulating vascular barrier integrity. $\alpha v\beta 5$-deficient mice have attenuated VEGF-induced vascular leak in the brain and skin,[21] and have reduced vascular leak in models of sepsis.[22] In addition, $\alpha v\beta 5$-deficient mice or mice treated with an $\alpha v\beta 5$ function-blocking antibody have attenuated vascular leak in acute lung injury.[23,24] Mechanistically it has been shown that $\alpha v\beta 5$ inhibition could prevent stress fiber formation in response to stimuli (*e.g.*, VEGF, IL1β, and LPS) and subsequently attenuate endothelial cell permeability.[22,23]

Given the role of $\alpha v\beta 5$ in regulating vascular permeability and its previously described function in models of acute injury, we sought to explore the role of $\alpha v\beta 5$ in the pathogenesis of IRI-induced AKI. Here we demonstrate that treatment with a function-blocking mAb specific for $\alpha v\beta 5$ attenuates AKI in a rat model of renal IRI. We further show that $\alpha v\beta 5$ inhibition attenuates microvascular permeability in this model. Analysis of $\alpha v\beta 5$ immunostaining reveals expression in perivascular cells of the kidney, including vascular smooth muscle cells (VSMCs) and pericytes. We demonstrate that blocking $\alpha v\beta 5$ can attenuate vascular leak in a three-dimensional microfluidic coculture system in a pericyte-dependent manner. Our data support a novel mechanism for $\alpha v\beta 5$ in mediating vascular permeability in AKI.

Results

Inhibition of $\alpha v\beta 5$ Integrin Reduces Renal Injury after IRI

A rat model of renal IRI was used to investigate the role of $\alpha v\beta 5$ integrin in AKI. Rats were treated with

two doses of a function-blocking *αvβ5* antibody (ALULA, previously described by Su *et al.*[23]), 18 hours preclamp and 30 hours post-ischemia. IRI produced a marked increase in serum creatinine in the control antibody-treated rats that was significantly reduced in the *αvβ5* antibody-treated rats (Figure 1A). Because no significant differences among the 10, 3, and 1 mg/kg doses of *αvβ5* antibody were detected, further experiments were conducted with lower doses of antibody and under these conditions a dose-response was observed (Figure 1B).

A single dose of *αvβ5* antibody administered 6 hours preclamp also significantly reduced serum creatinine levels at 24, 48, and 72 hours postinjury (Figure 2A). Effects of this single antibody dose were further evaluated using histopathologic end points. Composite lesion scores combining features of injury and regeneration were assessed by stereological analysis of hematoxylin and eosin–stained kidney sections. These correlated well with the serum creatinine results, with significant inhibition of lesions in the *αvβ5* antibody group observed at 72 hours post-ischemia (Figure 2B).

A major consequence of renal ischemia is tubular epithelial cell death.[25] Activated caspase-3 was used as a marker of cell death in kidney to investigate whether *αvβ5* inhibition modulates ischemia-induced epithelial cell loss. Activated caspase-3 levels in the renal medulla were found to be significantly reduced at 24 hours in the kidneys of *αvβ5* mAb-treated rats (Figure 3). The levels of additional injury markers *α*-smooth muscle actin and PDGFR*β* were also substantially reduced 72 hours post-ischemia with *αvβ5* inhibition, further supporting the protective effect of *αvβ5* inhibition during IRI (Supplemental Figures 1 and 2).

Expression Profiling Reveals Biomarkers of Renal Injury Are Decreased with *αvβ5* Blockade

To evaluate the effects of *αvβ5* inhibition on translatable biomarkers, we tested urine and serum collected post-IRI with the proteomic Rat KidneyMAP to evaluate the presence of proteins associated with renal injury. We identified two well established biomarkers, urinary KIM-1 and serum MCP-1 (Supplemental Figure 3), that exhibited patterns consistent with the biochemical and histologic indicators showing decreased injury with *αvβ5* antibody treatment.

Microarray analysis was performed on kidneys from control and *αvβ5* mAb-treated rats at 24 and 72 hours post-IRI, to explore the impact of *αvβ5* inhibition on global gene expression. Blockade of *αvβ5* resulted in 1460 and 604 transcripts differentially regulated at 24 and 72 hours compared with control antibody treatment, respectively. The differential expression of a subset of these genes was confirmed by quantitative PCR (Supplemental Table 1). Ingenuity Pathway Analysis revealed several biologic pathways impacted by *αvβ5* inhibition, including increased migration/differentiation of endothelial cells and increased proliferation of kidney cells with a concomitant decrease in immune cell recruitment and renal epithelial cell death (Table 1). In addition, markers of ischemic injury previously described in either rodent models of AKI or in human AKI, including KIM-1 (*havcr1*), Ngal (*lcn2*), and uromodulin (*umod*), were also altered by *αvβ5* inhibition (Figure 4). Ingenuity Upstream Regulator Analysis evaluated this gene expression dataset and predicted the inhibition of three signaling pathways involved in vascular permeability (IL1*β*, thrombin, and VEGF) as possible *αvβ5*-mediated molecular mechanisms in IRI (Supplemental Figure 4).

Integrin *αvβ5* Modulates Injury-Induced Vascular Permeability

The described role for *αvβ5* in vascular leak led us to examine the ability of *αvβ5* antibody treatment to attenuate vascular permeability after IRI. Intravital imaging was performed in rats 24 hours post-IRI using a rhodamine-conjugated albumin and a high molecular weight dextran to evaluate the microvascular permeability over time. We observed leakage of both the albumin and dextran from the renal microvasculature in the control antibody-treated animals. Leakage of both markers was also observed in the *αvβ5* mAb-treated animals. However, the extent of leakage in the *αvβ5* mAb-treated animals was

significantly less than that observed in the control antibody-treated animals (Figure 5).

In an effort to understand whether changes in renal blood flow would also contribute to the protection observed from *αvβ5* antibody treatment, we conducted additional intravital microscopy to evaluate red blood cell (RBC) flow rates. At 24 hours post-IRI there was no significant difference in RBC flow rates between control and *αvβ5* antibody-treated animals (Supplemental Figure 5), indicating that *αvβ5* inhibition does not alter cortical blood flow in IRI at this time point. This study does not rule out the possibility that *αvβ5* inhibition is altering blood flow at an earlier time point or altering flow in the outer medulla. Future studies should comprehensively address the possibility of *αvβ5*-mediated changes in blood flow and its contribution to the protection from vascular leak and injury observed with *αvβ5* antibody treatment.

Integrin *αvβ5* Expression in the Kidney

Previous studies report expression of *αvβ5* in multiple cell types *in vitro*[11–15]; however, there has not been an evaluation of the expression pattern in the kidney *in vivo*. To address the localization of *αvβ5* in the kidney, we generated an affinity-purified rabbit polyclonal antibody that could detect integrin *β5* in formalin-fixed paraffin-embedded tissue. Staining mouse kidneys with this antibody revealed broad expression of *αvβ5* in multiple regions of the kidney, including the glomerulus and cortical interstitium, and specificity of the staining was confirmed using *β5* null mouse tissue and competition with soluble *αvβ5* protein (Supplemental Figure 6, B and C).

To assess if *αvβ5* is present in renal perivascular and endothelial cells, we conducted immunofluorescence for *αvβ5*, PDGFR*β*, and CD31 on frozen tissue sections from mouse (Figure 6) and rat (Supplemental Figure 7). Our analysis suggests *αvβ5* is generally present on PDGFR*β*-expressing cells and is largely absent from CD31-expessing endothelial cells (Figure 6). The PDGFR*β* immunostaining also colocalized with NG2 (a proteoglycan expressed on pericytes and VSMCs), providing further evidence for *αvβ5* expression in perivascular cells (Supplemental Figure 8).

To identify any changes that injury may induce in the expression or localization of *αvβ5*, we immunostained rat kidneys 24 hours post-IRI. No substantial changes were detected in the levels of *αvβ5* expression or in its localization pattern post-IRI compared with an uninjured kidney (Supplemental Figure 7).

Integrin *αvβ5* Attenuates Vascular Leak in a Pericyte-Dependent Manner

To evaluate *αvβ5* antibody treatment in human kidney cells, we performed three-dimensional vascular permeability assays. Human renal endothelial cells were cultured in two different conditions: in the absence and presence of human kidney pericytes in a three-dimensional microfluidic device. As expected, treatment of the microvessels with thrombin significantly increased vascular permeability (P_d) in both the absence and presence of pericytes. Treatment with the *αvβ5* antibody had no significant effect on thrombin-induced permeability in endothelial cells alone (Figure 7A) but had a profound inhibitory effect on vascular leak in the coculture system (Figure 7B).

Quantitative PCR on cells from the microfluidic devices revealed substantially higher levels of *itgb5* mRNA in the kidney pericytes and in the coculture compared with endothelial cells alone, indicating that *β5* integrin expression is very low or absent in endothelial cells (Supplemental Figure 9).

Additional permeability studies were performed with LPS to demonstrate a broad role for *αvβ5* in regulating vascular permeability. As with thrombin, *αvβ5* inhibition also significantly inhibited LPS-induced permeability (Supplemental Figure 10A). F-actin staining in these devices revealed LPS treatment induces cytoskeletal disorganization, whereas normal cytoskeletal arrangements are largely preserved with

αvβ5 inhibition (Supplemental Figure 10B). These results suggest that *αvβ5* regulates vascular permeability in a pericyte-dependent manner.

Integrin *αvβ5* Is Important for Pericyte Adhesion and Migration

Integrins, including *αvβ5*, have a well defined role in regulating adhesion and migration in numerous cell types, and these processes could contribute to the function of pericytes in response to injury. To examine the contribution of *αvβ5* to pericyte adhesion we plated human kidney pericytes on either vitronectin (a known *αvβ5* ligand) or collagen (not an *αvβ5* ligand) in the presence or absence of antibody treatment. The *αvβ5* mAb led to a nearly 90% reduction in cell adhesion to vitronectin, but had no significant impact on adhesion to collagen (Figure 8A).

Migration studies were also performed using a scratch wound assay on human kidney pericytes on either collagen or vitronectin. Antibody treatment did not impact migration on collagen; however, on vitronectin, *αvβ5* antibody treatment significantly inhibited pericyte migration (Figure 8B). These studies demonstrate a ligand-dependent function for *αvβ5* in pericyte adhesion and migration, properties which are likely to contribute to the *αvβ5*-dependent function of pericytes in vascular permeability.

Postclamp Treatment with *αvβ5* Antibody Attenuates Injury Response

In order to evaluate the translational capacity of *αvβ5* inhibition, we employed a therapeutic dosing strategy. Rats were administered *αvβ5* antibody 8 hours postclamp release. This single therapeutic dose significantly reduced serum creatinine levels at 48 hours postinjury (Figure 9A). The effects of this dosing strategy were further evaluated using quantitative PCR of AKI biomarkers in kidneys isolated 72 hours post-IRI. *αvβ5* inhibition significantly reduced the expression of two biomarkers induced by injury (*havcr1*, *lcn2*) and increased the expression of two biomarkers diminished by injury (*umod*, *egf*). Together, these data demonstrate that treatment even several hours after ischemia may have therapeutic benefit.

Discussion

Here, we have shown that inhibition of integrin *αvβ5*, with a selective mAb, attenuates AKI in an IRI rat model. We further show that this antibody reduces vascular permeability, suggesting a mechanistic role for *αvβ5* in the pathogenesis of AKI. Importantly, we show that *αvβ5* is predominantly expressed in perivascular cells in the kidney, including pericytes. Using a novel three-dimensional microfluidic culture system we demonstrate for the first time a role for *αvβ5* function in pericytes leading to regulation of vascular leak. Importantly, inhibition of *αvβ5* hours after ischemia was still able to provide renal protection, indicating that this antibody could be a promising therapy for AKI.

The demonstration that *αvβ5* plays a key role in the kidney upon acute injury is consistent with previous data in other tissues, including protection from cerebral ischemia in *β5* null mice[21] and *αvβ5* inhibition resulting in reduced vascular leak in pulmonary ischemia.[24] Along with these *in vivo* studies, reports indicate that *αvβ5* is expressed in monolayer cultures of endothelial cells and that anti-*αvβ5* antibody treatment attenuates endothelial permeability.[22,23,26] In our studies, we evaluated the role of *αvβ5* in vascular leak using a three-dimensional microfluidic system that better mimics the *in vivo* structural and physiologic environment of the intact microvasculature. In this system, we observed that *αvβ5* does indeed play a key role in modulating vascular leak, but that this effect is largely dependent on pericytes. The reason for the experimental discrepancy between the three-dimensional system and the previous two-dimensional endothelial culture systems is uncertain, but there are numerous examples of three-dimensional culture systems better mimicking *in vivo* biology.[27] In addition to the three-dimensional microenvironment, the system we used incorporates flow. It is well established that vascular flow is critical for proper vascular barrier formation,[28,29] which is consistent with our observations that flow leads to a

much tighter barrier than observed in a static culture system (data not shown). Furthermore, it has been previously shown that pericytes are instrumental for proper vascular barrier function.[30] Likewise, in using this three-dimensional system we observe an improved barrier in the presence of pericytes. Taken together, this suggests that the three-dimensional system we have used more accurately recapitulates the biology of the microvascular barrier.

Consistent with a pericyte-dependent role for *αvβ5* in modulating vascular leak, we observe expression of *αvβ5* in perivascular cells of the kidney, including VSMCs and pericytes, whereas no detectable expression was observed in endothelial cells. Similarly, stromal cell-restricted expression of *αvβ5* in lung has also been observed (data not shown). Consistent with our results, previous studies evaluating *in situ* expression of *αvβ5* in the kidney have reported predominant mesangial cell expression in the glomerulus.[31]

Improved renal blood flow post-IRI is likely to have a protective effect on kidney function. The observed expression of *αvβ5* in VSMCs suggests there may be a mechanism whereby *αvβ5* inhibition ameliorates injury-induced vasoconstriction and improves blood flow. Our initial study using intravital microscopy to evaluate RBC flow in renal cortical vasculature post-IRI did not detect a significant difference in blood flow with *αvβ5* inhibition. However, it is important to note that this study does not rule out the possibility that *αvβ5* inhibition is altering blood flow at an earlier time point or altering flow in the outer medulla. Future studies that include a detailed time course analysis of blood flow throughout all phases of the injury could reveal another novel function for *αvβ5* and expand on the protective effects of *αvβ5* antibody treatment.

The *in vivo* immunostaining and *ex vivo* microfluidics studies suggest a role for *αvβ5* in pericytes, which are known to be critical for proper barrier function in the microvasculature.[32] This has been best studied in brain microvasculature where it has been shown that the absence of pericytes leads to breakdown of the blood–brain barrier.[33,34] In kidneys the role of pericytes in vascular leak has not been studied. In the context of acute injury in the kidney, pericytes can differentiate into αSMA-positive myofibroblasts and play a key role in contributing to the fibrotic response.[35] Recent work has shown that ablation of pericytes in the kidney leads to a rapid AKI, peritubular capillary loss, and lethality,[36] supporting the role of pericytes in maintaining normal kidney function. A key area of study will be to explore the precise cellular role of *αvβ5* in pericytes that contribute to its role in AKI.

To begin to understand this we have evaluated some functions of *αvβ5* in pericytes *in vitro*. We have shown that *αvβ5* is instrumental for pericyte adhesion as well as migration on a vitronectin substrate, a known *αvβ5* ligand. Vitronectin has been associated with the pathogenesis of several disease processes including neointimal formation in blood vessels,[37] liver cirrhosis,[38] diabetic nephropathy,[39] and CKD.[40] This involvement of vitronectin with disease states lends potential biologic significance to the regulation of pericyte migration on this substrate.

It has been proposed that pericytes may migrate from endothelial cells after ischemic injury[1] and it is plausible that this migration may contribute to the vascular permeability in renal IRI. In addition, pericyte migration away from the vasculature is thought to result in their differentiation to myofibroblasts.[8,35,41] By impairing the ability of pericytes to migrate, *αvβ5* inhibition could maintain pericyte–endothelial interactions, resulting in reduced vascular leak and diminished myofibroblast differentiation. This is supported by the reduced myofibroblast expansion observed with *αvβ5* inhibition. This suggests that *αvβ5* antibody could potentially protect from longer-term damage like the renal fibrosis that occurs in the weeks and months after AKI (reviewed in Ferenbach and Bonventre[1]).

Overall, our data highlight an important role for *αvβ5* in the pathogenesis of AKI and suggests that targeting this integrin to attenuate vascular permeability could provide an effective therapy, one that is mechanistically highly differentiated from other therapeutic approaches that have failed in the clinic

setting.

Concise Methods

Unilateral Clamp Ischemia Model

Animal experiments were approved by the Indiana University School of Medicine Institutional Animal Care and Use Committee. Male Sprague Dawley rats (Harlan Laboratories) were anesthetized with isoflurane and placed on a warming pad for temperature maintenance. The right kidney was removed and the renal artery and vein sutured off. Ischemia of the left kidney was initiated by clamping the renal artery and vein for 30 minutes using nontraumatic clamps (Fine Scientific Tools). At the conclusion of the ischemic period, the clamps were removed and the kidneys were observed to insure rapid re-establishment of blood flow. The *αvβ5* blocking antibody (ALULA) used in these studies was previously described.[23] The 2H6 mouse IgG2b mAb was used as a control. Antibodies were administered at a volume of 300 μl by subcutaneous injection at defined times before clamping.

Immunostaining of Fixed Kidneys

To detect *αvβ5* in formalin-fixed, paraffin-embedded tissues, a human *β5* integrin-specific polyclonal antiserum was prepared by immunizing a rabbit with purified soluble human *αvβ5* ectodomain protein generated with recombinant constructs in CHO cells. The total IgG fraction was purified from the antiserum using protein-A affinity chromatography, and subjected to affinity depletion using Sepharose beads conjugated to soluble human *αvβ6* protein, in order to remove human *α*v-reactive components. The human *β5*-integrin specific rabbit antibodies were then affinity purified using Sepharose beads conjugated to soluble human *αvβ5* protein. The final isolated rabbit IgG fraction was only reactive to human *β5*-containing integrin but not any other integrin subunits, as tested by ELISA (data not shown). Formalin-fixed tissues were embedded in paraffin, sectioned at 5 μM, and processed on the Ventana Discovery XT platform (Roche) using the purified anti-human *β5* polyclonal antibody. Immunohistochemistry of additional markers was performed as above, using the following antibodies: PDGFR*β* (Thermo Fisher), *α*-smooth muscle actin (*α*SMA; Abcam, Inc.), and activated caspase-3 (Cell Signaling Technology). Quantification of caspase-3 immunoreactive area was accomplished by custom-designing algorithms in Visiopharm (Denmark) software.

Additional immunostaining for *αvβ5* was performed on frozen tissue from rat (Sprague–Dawley strain; Harlan/ENVIGO) and mouse (*Itgb5*^{tm1Des} *β5* null strain and wild-type 129 SvJ strain; Jackson Laboratories). Tissues were fixed in 4% PFA and embedded in OTC (Electron Microscopy Sciences). Frozen blocks were sectioned on a cryostat at 10–20 μm thickness and slides were stored at −80°C. Primary and secondary antibodies were as follows: *αvβ5* antibody ALULA[23] (humanized variant), mouse anti-rat CD31 or rat anti-mouse CD31 (eBioscience), rabbit anti-PDGFRb (clone 28E1; Cell Signaling Technology), mouse anti-rat NG2 (Abcam, Inc.), anti-human Cy3 (Jackson ImmunoResearch), anti-rabbit AF647, anti-rat AF488, and anti-mouse AF488 (Life Technologies). Images were acquired on a Marianas confocal system (3i) at submicron *z*-axis resolution. Three-dimensional image stacks were pseudocolored and reconstructed with Volocity (Perkin-Elmer).

Histologic Evaluation

Hematoxylin and eosin–stained sections from formalin-fixed, paraffin-embedded kidneys were examined by a blinded, board certified veterinary pathologist for injury and regeneration using a scoring method modified from Kelleher et al.[42] The following criteria were scored: (*1*) injury score: tubular necrosis, calcific debris in tubular lumina, interstitial inflammation, casts, juxta-glomerular apparatus prominence, interstitial edema, brush border loss, tubular proteinosis, and pelvic congestion; and (*2*) regeneration score:

neutrophils in vasa recti, tubular regeneration, and tubular cell mitoses. Lesions were scored on a scale of 0–2 (0, none; 0.5, minimal; 1, mild; 1.5 moderate; and 2, marked). Composite lesion scores presented are a combination of the injury and regeneration scores.

Serum and Urine Biomarker Measurements

Serum creatinine was measured at baseline and at days 1, 2, and 3 postclamp (animals euthanized at 24 hours postclamp have only baseline and day 1 serum creatinine measurements). Levels were measured using an AU480 Chemistry Analyzer (Beckman) and reported as milligram per deciliter. Profiling of serum and urine biomarkers of renal injury was conducted using the Luminex Bead assay platform with the multianalyte panel Rat KidneyMAP v1.0 (Myriad RBM).

RNA Isolation, Microarray Analysis, and Quantitative PCR

Total RNA from the kidney was isolated in QIAzol (Qiagen) using mechanical disruption on the FastPrep system (MP Biomedical), and purified using the RNeasy Mini Kit (Qiagen). RNA was quantitated (NanoDrop; Thermo Fisher) and was evaluated for integrity using the RNA 6000 Nano Assay on a Bioanalyzer 2100 (Agilent).

Gene expression microarray experiments were performed at Expression Analysis (a Quintiles company) as follows. Total RNA was labeled and hybridized using the Ambion WT Expression kit according to the manufacturer's instructions. After hybridization, arrays were washed and stained using standard Affymetrix procedures before scanning on the Affymetrix GeneChip Scanner. For differential expression analysis, a two-group analysis was performed using the comparative method Permutation Analysis for Differential Expression to develop false discovery rate-based estimates of groups of genes using a shrunken t-statistic. A false discovery rate of <0.05 and a fold change of >1.5 (control antibody-treated versus $\alpha v\beta 5$ antibody-treated) was considered significant.

For quantitative PCR confirmation of microarray results, cDNA was synthesized from 1 μg of RNA using the SuperScript VILO cDNA Synthesis Kit (Thermo Fisher) and quantitative PCR was performed using Taqman Gene Expression assays run on the QuantStudio 7 (Thermo Fisher). Ct values of target genes were normalized to the *eif1a* control gene to generate ΔCt values.

Intravital Microscopy to Evaluate Vascular Permeability and RBC Flow *In Vivo*

Rat serum albumin was conjugated to Texas Red as previously described (TR-RSA).[43] A 150 kD fluorescein conjugated dextran (TdB Consultancy) was dissolved in normal saline. To remove any small molecular weight components, the stock solution was dialyzed against normal saline using a 100 kD MWCO Spectra-Por Float-A-Lyzer membrane (Thermo Fisher).

Images were acquired using an Olympus FV-1000 microscope, with an original magnification of ×60, 1.2NA water immersion objective, and highly sensitive GaAsP nondescanned (external) detectors. Ten random fields were marked and imaged at 5, 15, and 30 minutes postinfusion of the dual TR-RSA/150 kD fluorescein dextran bolus. All of the images were taken approximately 5–10 μm below the kidney capsule where interstitial space is prevalent.

The degree of extravasation of the two different molecular mass markers (approximately 66 kDa for the TR-RSA and 150 kDa for the fluorescein-dextran) was used examine the severity of damage to vascular integrity. TR-RSA was used to rank mild to moderate vascular damage and the 150 kD fluorescein-dextran was used to rank more severe damage (see Supplemental Material for details). A score of 0 indicates that no amount of the compound is present in the interstitial space. A score of 1 is given to an image where some amount of the compound is seen in the interstitial space of a small region of the total image. A score

of 2 is given to an image where the compound leaks into the interstitial space of the majority of the image. A score of 3 is given to an image where the concentration of the compound in the interstitial space starts to match the intensities seen in the circulating microvasculature. This is indicative of severe damage particularly for TR-RSA at 5 and 15 minute time points or the 150 kD fluorescein-dextran at any time point.

RBC velocity was calculated as previously described.[44] Briefly, utilizing the 150 kD dextran retained in the vasculature, RBC velocity was determined from single plane images or line scans as the dextran labels only the plasma and is excluded from RBC and white blood cells causing them to appear as dark streaks. This was accomplished by determination of the slope induced during image acquisition of the RBCs; faster moving RBC produce a shallower slope while slower moving RBCs produce a steeper slope. Speed was calculated by using the dimensions of time (the *y*-axis) and distance (the *x*-axis).

Microfluidic Platform for Vascular Permeability

To determine the permeability of endothelial monolayers and endothelial-pericyte co-cultures *in vitro*, microvessels were formed in microfluidic devices as described previously.[45] Human renal glomerular endothelial cells (ScienCell) (and in specified cases, human renal pericytes) were seeded in 160 μm diameter tubes formed in collagen type I hydrogels to create lumenized microvessels, and 70 kD dextran was perfused through the vessel lumens to quantify the diffusive permeability.[46]

In Vitro Pericyte Adhesion Assay

Costar 96-well high binding plates were coated overnight at 4°C with 0.1% collagen (Sigma) or 10 μg/ml vitronectin in PBS (R&D Systems). Plates were washed then blocked for 1 hour at 37°C and washed with buffer again. Antibodies (10 μg/ml) 2H6, anti-αVβ5, and anti-αVβ3 (MAB1976; Millipore) were added to wells prior to cell seeding. Human fetal kidney pericytes were fluorescently labeled with Calcein-AM (Molecular Probes) and seeded into antibody-containing wells. After incubation, plates were washed then read on a Synergy ^{1}H microplate reader (BioTek) to quantify adherent cells via fluorescent intensity.

Scratch Wound Migration Assay

Essen Bioscience 96-well ImageLock plates were coated overnight at 4°C with 0.1% collagen (Sigma) or 10 μg/ml vitronectin in PBS (R&D Systems), then washed with PBS. Human fetal kidney pericytes were seeded in Opti-MEM (Thermo Fisher) and incubated at 37°C for 6 hours prior to scratch using the Woundmaker (Essen Bioscience). Antibodies 2H6, anti-αVβ5, anti- αVβ3 (MAB1976; Millipore), or a JNK inhibitor (Selleckchem SP600125) were added to the wells 1 hour before scratch. Plates were imaged in the Incucyte ZOOM system (Essen Bioscience) every 2 hours for 48 hours. An analysis was run on each plate and wound confluence was calculated at each individual time point for each treatment condition.

Statistical Analyses

GraphPad Prism 6 (GraphPad Inc.) was used to analyze the data. Data were analyzed by two-tailed *t* test or two- or one-way ANOVA with *post hoc* analysis as appropriate. $P<0.05$ was used to indicate significance.

Disclosures

J.E.C., C.Q., I.G.G., J.D., B.M.D., S.M., J.W.M, J.S.D., and M.A.C. are former employees of Biogen, and A.T.M., T.L.R., G.M., A.H., F.Q., P.H.W. and S.M.V. are currently employees of and stockholders in Biogen. This does not alter the authors' adherence to all the policies of the *Journal of the American Society of Nephrology* on sharing data and materials.

Supplementary Material

Supplemental Data:

Acknowledgments

This work was supported by the following National Institutes of Health grants (to C.S.C.): EB00262, EB017103, HL115553, HL119346, and the Biogen Fibrosis Consortium.

Footnotes

Published online ahead of print. Publication date available at www.jasn.org.

This article contains supplemental material online at http://jasn.asnjournals.org/lookup/suppl/doi:10.1681/ASN.2016020200/-/DCSupplemental.

References

1. Ferenbach DA, Bonventre JV.: Mechanisms of maladaptive repair after AKI leading to accelerated kidney ageing and CKD. Nat Rev Nephrol 11: 264–276, 2015 [PMCID: PMC4412815] [PubMed: 25643664]

2. Coca SG, Singanamala S, Parikh CR.: Chronic kidney disease after acute kidney injury: A systematic review and meta-analysis. Kidney Int 81: 442–448, 2012 [PMCID: PMC3788581] [PubMed: 22113526]

3. Wonnacott A, Meran S, Amphlett B, Talabani B, Phillips A.: Epidemiology and outcomes in community-acquired versus hospital-acquired AKI. Clin J Am Soc Nephrol 9: 1007–1014, 2014 [PMCID: PMC4046725] [PubMed: 24677557]

4. Sharfuddin AA, Molitoris BA.: Pathophysiology of ischemic acute kidney injury. Nat Rev Nephrol 7: 189–200, 2011 [PubMed: 21364518]

5. Sutton TA: Alteration of microvascular permeability in acute kidney injury. Microvasc Res 77: 4–7, 2009 [PMCID: PMC2680138] [PubMed: 18938184]

6. Sutton TA, Mang HE, Campos SB, Sandoval RM, Yoder MC, Molitoris BA.: Injury of the renal microvascular endothelium alters barrier function after ischemia. Am J Physiol Renal Physiol 285: F191–F198, 2003 [PubMed: 12684225]

7. Goddard LM, Iruela-Arispe ML.: Cellular and molecular regulation of vascular permeability. Thromb Haemost 109: 407–415, 2013 [PMCID: PMC3786592] [PubMed: 23389236]

8. Kramann R, Humphreys BD.: Kidney pericytes: Roles in regeneration and fibrosis. Semin Nephrol 34: 374–383, 2014 [PMCID: PMC4163198] [PubMed: 25217266]

9. Felding-Habermann B, Cheresh DA.: Vitronectin and its receptors. Curr Opin Cell Biol 5: 864–868, 1993 [PubMed: 7694604]

10. Akakura S, Singh S, Spataro M, Akakura R, Kim J-I, Albert ML, Birge RB.: The opsonin MFG-E8 is a ligand for the alphavbeta5 integrin and triggers DOCK180-dependent Rac1 activation for the phagocytosis of apoptotic cells. Exp Cell Res 292: 403–416, 2004 [PubMed: 14697347]

11. Uehara K, Uehara A.: Integrin *αvβ5* in endothelial cells of rat splenic sinus: An immunohistochemical and ultrastructural study. Cell Tissue Res 356: 183–193, 2014 [PubMed: 24556923]

12. Pasqualini R, Bodorova J, Ye S, Hemler ME.: A study of the structure, function and distribution of beta

5 integrins using novel anti-beta 5 monoclonal antibodies. J Cell Sci 105: 101–111, 1993 [PubMed: 7689573]

13. Conron M, Bondenson J, Pantelidis P, Beynon HLC, Feldmann M, du Bois RM, Foxwell BM.: Alveolar macrophages and T cells from sarcoid, but not normal lung, are permissive to adenovirus infection and allow analysis of NF- κ B–dependent signaling pathways. Am J Res Mol Bio 25: 1–9, 2001 [PubMed: 11509322]

14. Bianchi-Smiraglia A, Kunnev D, Limoge M, Lee A, Beckerle MC, Bakin AV.: Integrin-*β*5 and zyxin mediate formation of ventral stress fibers in response to transforming growth factor *β*. Cell Cycle 12: 3377–3389, 2013 [PMCID: PMC3895427] [PubMed: 24036928]

15. Sarrazy V, Koehler A, Chow ML, Zimina E, Li CX, Kato H, Caldarone CA, Hinz B.: Integrins *αvβ*5 and *αvβ*3 promote latent TGF-*β*1 activation by human cardiac fibroblast contraction. Cardiovasc Res 102: 407–417, 2014 [PMCID: PMC4030512] [PubMed: 24639195]

16. Eliceiri BP, Cheresh DA.: The role of alphav integrins during angiogenesis: Insights into potential mechanisms of action and clinical development. J Clin Invest 103: 1227–1230, 1999 [PMCID: PMC408360] [PubMed: 10225964]

17. Albert ML, Kim JI, Birge RB.: alphavbeta5 integrin recruits the CrkII-Dock180-rac1 complex for phagocytosis of apoptotic cells. Nat Cell Biol 2: 899–905, 2000 [PubMed: 11146654]

18. Huang S, Endo RI, Nemerow GR.: Upregulation of integrins alpha v beta 3 and alpha v beta 5 on human monocytes and T lymphocytes facilitates adenovirus-mediated gene delivery. J Virol 69: 2257–2263, 1995 [PMCID: PMC188895] [PubMed: 7533853]

19. Khalifeh-Soltani A, McKleroy W, Sakuma S, Cheung YY, Tharp K, Qiu Y, Turner SM, Chawla A, Stahl A, Atabai K.: Mfge8 promotes obesity by mediating the uptake of dietary fats and serum fatty acids. Nat Med 20: 175–183, 2014 [PMCID: PMC4273653] [PubMed: 24441829]

20. Nandrot EF, Kim Y, Brodie SE, Huang X, Sheppard D, Finnemann SC.: Loss of synchronized retinal phagocytosis and age-related blindness in mice lacking alphavbeta5 integrin. J Exp Med 200: 1539–1545, 2004 [PMCID: PMC2211990] [PubMed: 15596525]

21. Eliceiri BP, Puente XS, Hood JD, Stupack DG, Schlaepfer DD, Huang XZ, Sheppard D, Cheresh DA.: Src-mediated coupling of focal adhesion kinase to integrin alpha(v)beta5 in vascular endothelial growth factor signaling. J Cell Biol 157: 149–160, 2002 [PMCID: PMC2173263] [PubMed: 11927607]

22. Su G, Atakilit A, Li JT, Wu N, Luong J, Chen R, Bhattacharya M, Sheppard D.: Effective treatment of mouse sepsis with an inhibitory antibody targeting integrin *αvβ*5. Crit Care Med 41: 546–553, 2013 [PubMed: 23263571]

23. Su G, Hodnett M, Wu N, Atakilit A, Kosinski C, Godzich M, Huang XZ, Kim JK, Frank JA, Matthay MA, Sheppard D, Pittet J-F.: Integrin alphavbeta5 regulates lung vascular permeability and pulmonary endothelial barrier function. Am J Respir Cell Mol Biol 36: 377–386, 2007 [PMCID: PMC1899321] [PubMed: 17079779]

24. Ganter MT, Roux J, Miyazawa B, Howard M, Frank JA, Su G, Sheppard D, Violette SM, Weinreb PH, Horan GS, Matthay MA, Pittet J-F.: Interleukin-1beta causes acute lung injury via alphavbeta5 and alphavbeta6 integrin-dependent mechanisms. Circ Res 102: 804–812, 2008 [PMCID: PMC2739091] [PubMed: 18276918]

25. Havasi A, Borkan SC.: Apoptosis and acute kidney injury. Kidney Int 80: 29–40, 2011 [PMCID: PMC4625984] [PubMed: 21562469]

26. Bae J-S, Lee W, Nam J-O, Kim J-E, Kim S-W, Kim I-S.: Transforming growth factor *β*-induced protein promotes severe vascular inflammatory responses. Am J Respir Crit Care Med 189: 779–786, 2014 [PubMed: 24506343]

27. Kelly EJ, Wang Z, Voellinger JL, Yeung CK, Shen DD, Thummel KE, Zheng Y, Ligresti G, Eaton DL, Muczynski KA, Duffield JS, Neumann T, Tourovskaia A, Fauver M, Kramer G, Asp E, Himmelfarb J.: Innovations in preclinical biology: Ex vivo engineering of a human kidney tissue microperfusion system. Stem Cell Res Ther 4[Suppl1]: S17, 2013 [PMCID: PMC4029535] [PubMed: 24564863]

28. Gulino-Debrac D: Mechanotransduction at the basis of endothelial barrier function. Tissue Barriers 1: e24180, 2013 [PMCID: PMC3879236] [PubMed: 24665386]

29. Deosarkar SP, Prabhakarpandian B, Wang B, Sheffield JB, Krynska B, Kiani MF.: A novel dynamic neonatal blood-brain barrier on a chip. PLoS One 10: e0142725, 2015 [PMCID: PMC4640840] [PubMed: 26555149]

30. Armulik A, Genové G, Mäe M, Nisancioglu MH, Wallgard E, Niaudet C, He L, Norlin J, Lindblom P, Strittmatter K, Johansson BR, Betsholtz C.: Pericytes regulate the blood-brain barrier. Nature 468: 557–561, 2010 [PubMed: 20944627]

31. Hafdi Z, Lesavre P, Nejjari M, Halbwachs-Mecarelli L, Droz D, Noël LH.: Distribution of *αvβ*T3, *αvβ*TB5 integrins and the Integrin Associated Protein — IAP (CD47) in human glomerular diseases. Cell Commun Adhes 7: 441–451, 2000 [PubMed: 11051455]

32. Winkler EA, Bell RD, Zlokovic BV.: Central nervous system pericytes in health and disease. Nat Neurosci 14: 1398–1405, 2011 [PMCID: PMC4020628] [PubMed: 22030551]

33. Bell RD, Winkler EA, Sagare AP, Singh I, LaRue B, Deane R, Zlokovic BV.: Pericytes control key neurovascular functions and neuronal phenotype in the adult brain and during brain aging. Neuron 68: 409–427, 2010 [PMCID: PMC3056408] [PubMed: 21040844]

34. Edelman DA, Jiang Y, Tyburski J, Wilson RF, Steffes C.: Pericytes and their role in microvasculature homeostasis. J Surg Res 135: 305–311, 2006 [PubMed: 16930620]

35. Chen YT, Chang FC, Wu CF, Chou YH, Hsu HL, Chiang WC, Shen J, Chen YM, Wu KD, Tsai TJ, Duffield JS, Lin SL.: Platelet-derived growth factor receptor signaling activates pericyte-myofibroblast transition in obstructive and post-ischemic kidney fibrosis. Kidney Int 80: 1170–1181, 2011 [PubMed: 21716259]

36. Lemos DR, Marsh G, Huang A, Campanholle G, Aburatani T, Dang L, Gomez I, Fisher K, Ligresti G, Peti-Peterdi J, Duffield JS.: Maintenance of vascular integrity by pericytes is essential for normal kidney function. Am J Physiol Renal Physiol 311: F1230–F1242, 2016 [PMCID: PMC5210201] [PubMed: 27335372]

37. Dufourcq P, Couffinhal T, Alzieu P, Daret D, Moreau C, Duplàa C, Bonnet J.: Vitronectin is up-regulated after vascular injury and vitronectin blockade prevents neointima formation. Cardiovasc Res 53: 952–962, 2002 [PubMed: 11922905]

38. Koukoulis GK, Shen J, Virtanen I, Gould VE.: Vitronectin in the cirrhotic liver: an immunomarker of mature fibrosis. Hum Pathol 32: 1356–1362, 2001 [PubMed: 11774169]

39. Yoon S, Gingras D, Bendayan M.: Alterations of vitronectin and its receptor alpha(v) integrin in the rat renal glomerular wall during diabetes. Am J Kidney Dis 38: 1298–1306, 2001 [PubMed: 11728964]

40. López-Guisa JM, Rassa AC, Cai X, Collins SJ, Eddy AA.: Vitronectin accumulates in the interstitium

but minimally impacts fibrogenesis in experimental chronic kidney disease. Am J Physiol Renal Physiol 300: F1244–F1254, 2011 [PMCID: PMC3094052] [PubMed: 21270094]

41. Humphreys BD, Lin SL, Kobayashi A, Hudson TE, Nowlin BT, Bonventre JV, Valerius MT, McMahon AP, Duffield JS.: Fate tracing reveals the pericyte and not epithelial origin of myofibroblasts in kidney fibrosis. Am J Pathol 176: 85–97, 2010 [PMCID: PMC2797872] [PubMed: 20008127]

42. Kelleher SP, Robinette JB, Miller F, Conger JD.: Effect of hemorrhagic reduction in blood pressure on recovery from acute renal failure. Kidney Int 31: 725–730, 1987 [PubMed: 3573537]

43. Sandoval RM, Wagner MC, Patel M, Campos-Bilderback SB, Rhodes GJ, Wang E, Wean SE, Clendenon SS, Molitoris BA.: Multiple factors influence glomerular albumin permeability in rats. J Am Soc Nephrol 23: 447–457, 2012 [PMCID: PMC3294301] [PubMed: 22223875]

44. Sharfuddin AA, Sandoval RM, Molitoris BA.: Imaging techniques in acute kidney injury. Nephron Clin Pract 109: c198–c204, 2008 [PubMed: 18802368]

45. Nguyen DH, Stapleton SC, Yang MT, Cha SS, Choi CK, Galie PA, Chen CS.: Biomimetic model to reconstitute angiogenic sprouting morphogenesis in vitro. Proc Natl Acad Sci U S A 110: 6712–6717, 2013 [PMCID: PMC3637738] [PubMed: 23569284]

46. Adamson RH, Lenz JF, Curry FE.: Quantitative laser scanning confocal microscopy on single capillaries: permeability measurement. Microcirculation 1: 251–265, 1994 [PubMed: 8790594]

Figures and Tables

Figure 1.

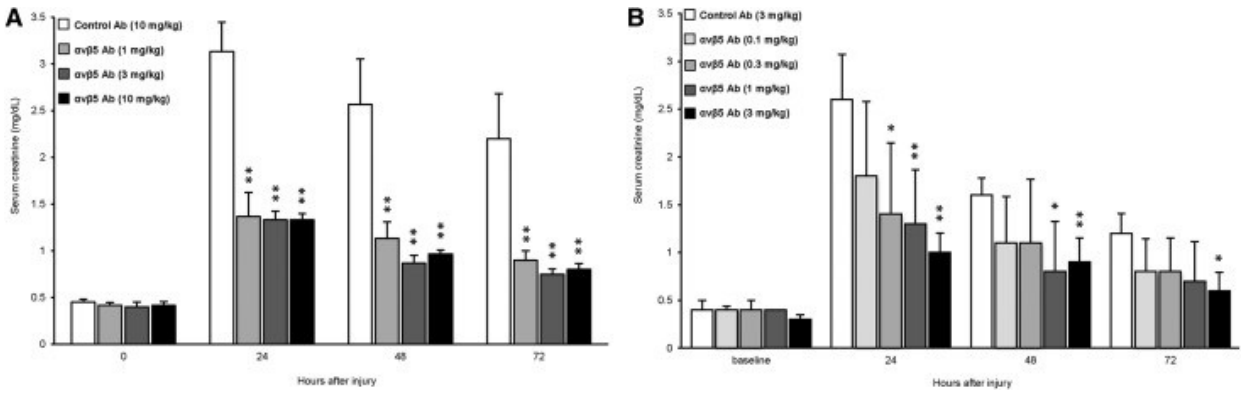

Treatment with *αvβ5* mAb protects kidneys in a rat model of renal IRI. To establish the dose-response efficacy of an *αvβ5*-blocking antibody (*αvβ5* antibody), rats were treated with (A) 10, 3, or 1 mg/kg or (B) 3, 1, 0.3, or 0.1 mg/kg at 18 hours pre- and 30 hours post-clamp. Doses of 10 and 3 mg/kg were equally effective in attenuating ischemia-induced serum creatinine increases at 24, 48, and 72 hours post-injury. **P*<0.05; ***P*<0.01 versus control antibody; error bars = SEM.

Figure 2.

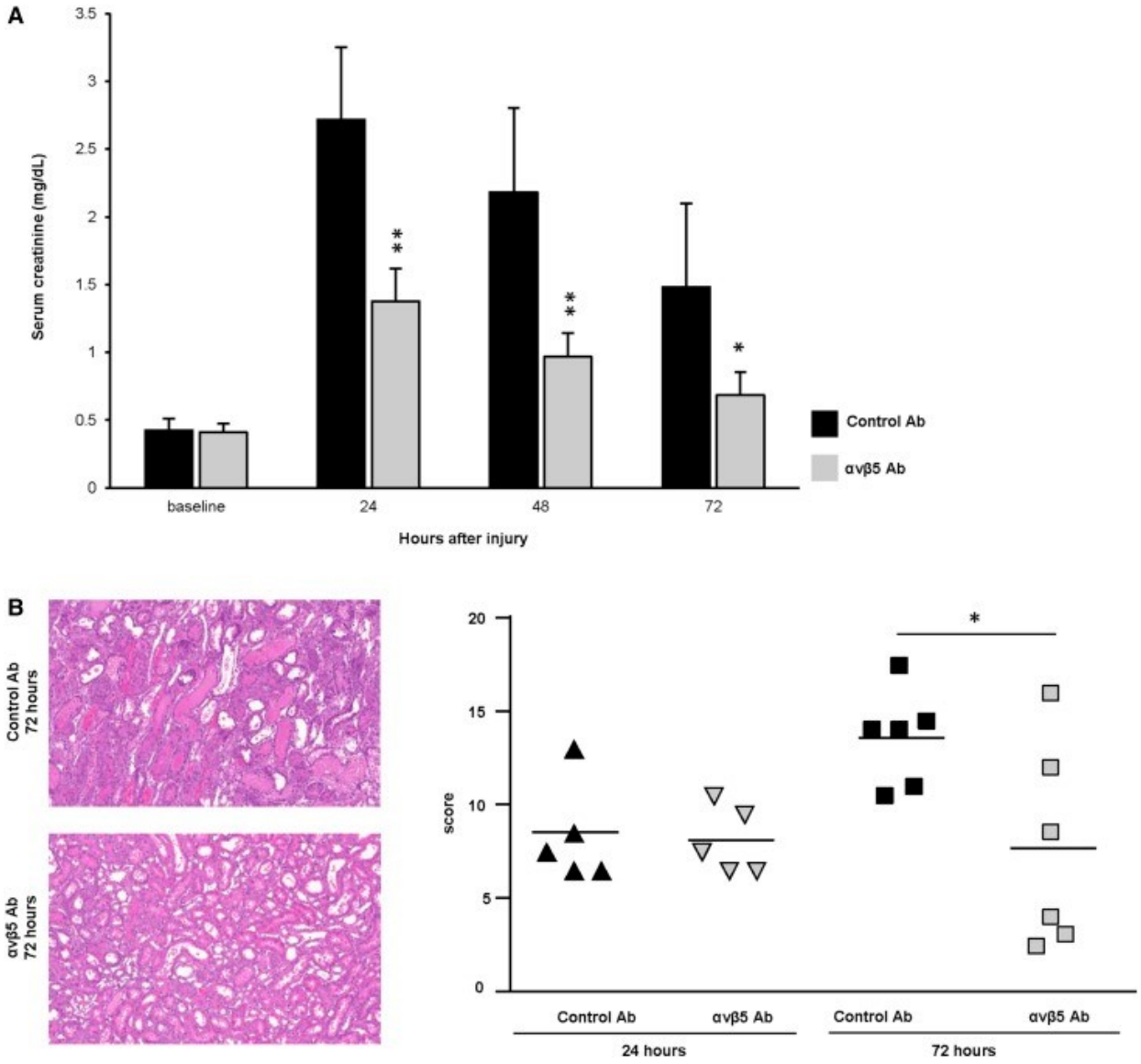

Single dose of *αvβ5* antibody improves kidney function and reduces tubular injury. (A) Rats were treated with a single dose (3 mg/kg) of *αvβ5* antibody 6 hours before ischemic injury. This single dose was effective in attenuating ischemia-induced serum creatinine increases at 24, 48, and 72 hours postinjury. **P*<0.05; ***P*<0.01 versus control antibody; error bars = SEM. (B) Kidneys were harvested at 24 and 72 hours postclamp from the study in A. Histopathologic examination of hematoxylin and eosin–stained kidney sections utilized several morphologic features to generate a composite lesion score (see Concise Methods for details). Rats treated with *αvβ5* antibody had a significantly lower score at 72 hours post-IRI. **P*<0.05 compared with control antibody.

Figure 3.

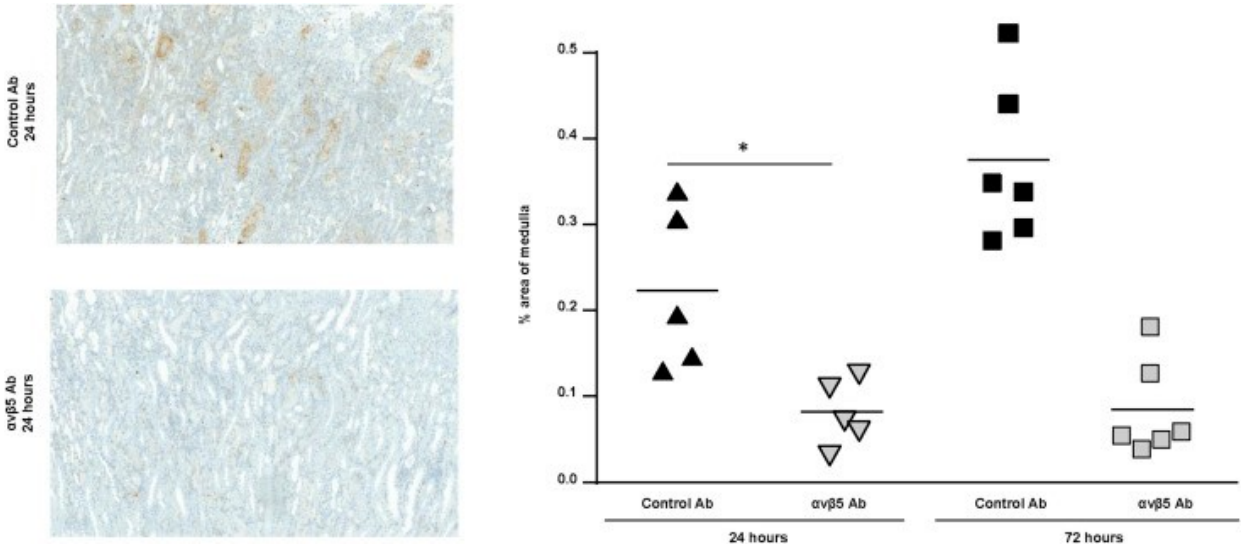

αvβ5 inhibition decreases ischemia-induced apoptosis. Kidneys were harvested at 24 and 72 hours postclamp after a single dose (3 mg/kg) of *αvβ5* antibody 6 hours preclamp. Activated capsase-3 was used as a measure of apoptosis in post-IRI kidney sections. The degree of caspase-3 immunoreactivity was quantified and calculated as a percent area of medulla. Rats treated with *αvβ5* antibody had significantly reduced apoptosis in the renal medulla at 24 hours postinjury. **P*<0.05 compared with control antibody.

Table 1.

Selected pathways regulated by *αvβ5* inhibition

Function Annotation	*P* Value	*Z*-Score	Predicted Activation
Angiogenesis	3.11E-05	2.574	Increased
Migration of endothelial cells	1.66E-04	2.335	Increased
Differentiation of endothelial cells	3.34E-05	1.893	Increased
Kidney development	9.52E-03	1.676	Increased
Proliferation of kidney cells	2.57E-02	1.580	Increased
Apoptosis of renal epithelial cells	1.10E-03	−2.011	Decreased
Failure of kidney	7.16E-06	−2.126	Decreased
Adhesion of immune cells	2.10E-04	−2.298	Decreased
Atrophy of renal tubule	1.62E-04	−2.414	Decreased
Fibrosis	2.23E-06	−2.498	Decreased
Recruitment of immune cells	1.12E-05	−2.555	Decreased
Hydronephrosis	6.94E-07	−2.600	Decreased

Ingenuity Pathway Analysis was performed on transcripts differentially expressed at 24 and 72 hours post-IRI with *αvβ5* antibody compared with control antibody (fold change >1.5; false discovery rate <0.05). Ingenuity Pathway Analysis *Z*-scores >1.5 or <−1.5 predicted increased or decreased activation of biologic functions with *αvβ5* inhibition.

Figure 4.

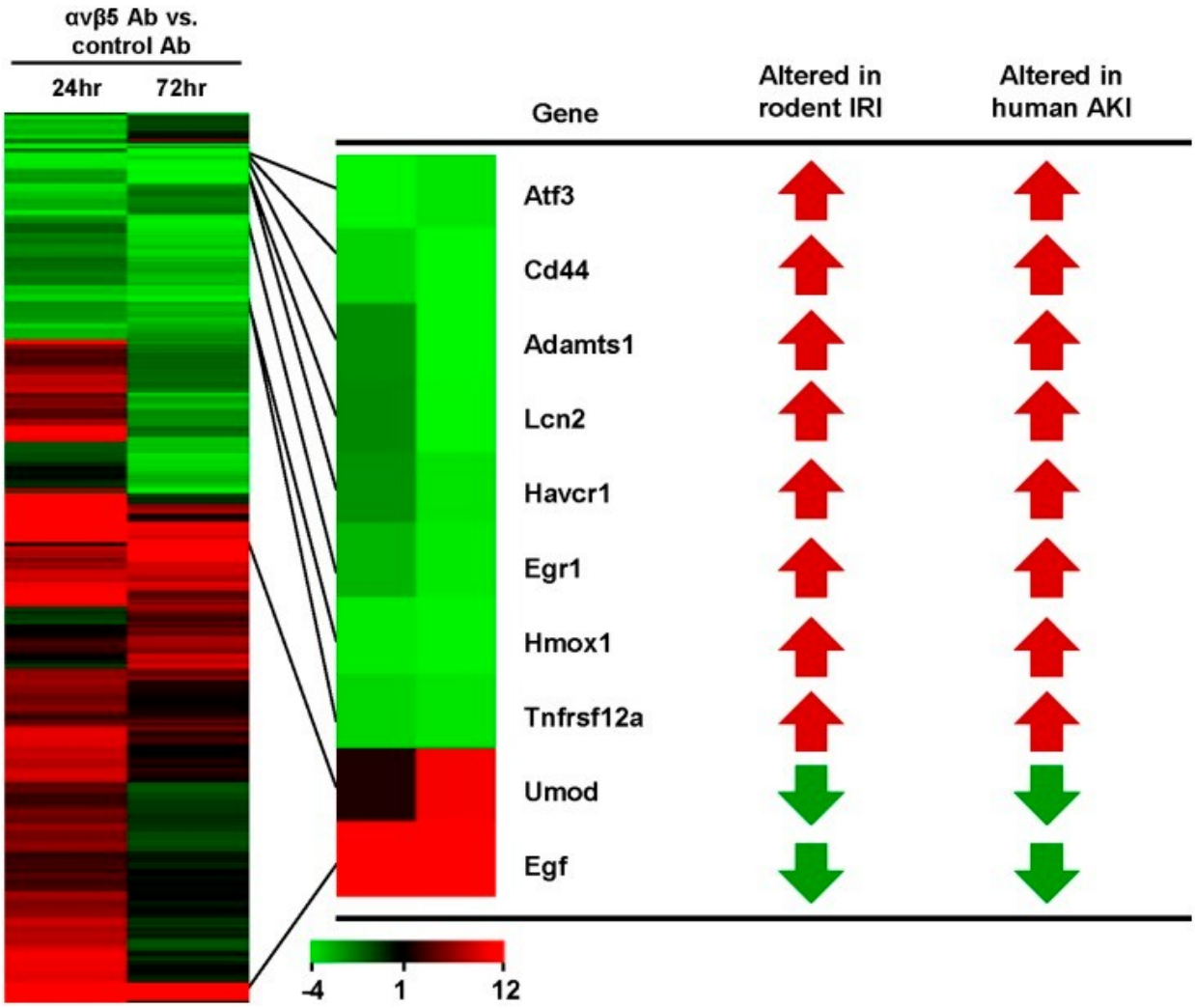

Profiling of kidney reveals previously identified genes in rodent and human AKI are altered with *αvβ5* inhibition. Heat map depicts transcripts differentially expressed at 24 or 72 hours post-IRI with *αvβ5* antibody treatment compared with control antibody treatment. Table includes genes previously identified as altered in rodent IR models and in human AKI that were oppositely regulated with *αvβ5* antibody treatment.

Figure 5.

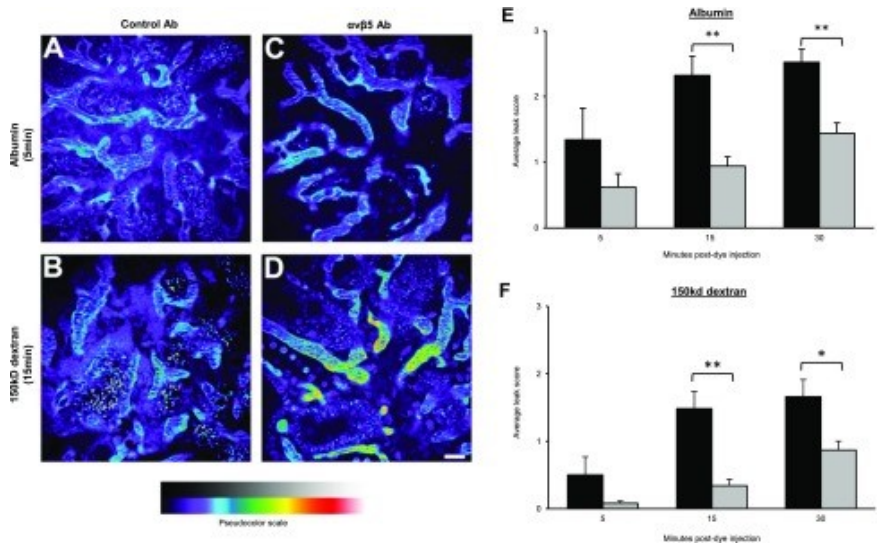

αvβ5 inhibition reduces vascular leak after injury. (A) Texas Red-conjugated albumin and a 150 kD fluorescein-dextran were intravenously coinjected into rats at 24 hours post-ischemia to evaluate microvascular permeability after injury. Intravital imaging of the cortex revealed leakage of both the albumin and the high molecular weight dextran from the renal microvasculature in the control antibody-treated animals (A and B), and this leak was substantially reduced in the *αvβ5* antibody-treated animals (C and D). The images were scored for degree of extravasation and the average leak scores for albumin (E) and the 150 kD dextran (F) were calculated. **P*<0.05; ***P*<0.01 versus control antibody; error bars = SEM; image dimensions = 212×212 μm.

Figure 6.

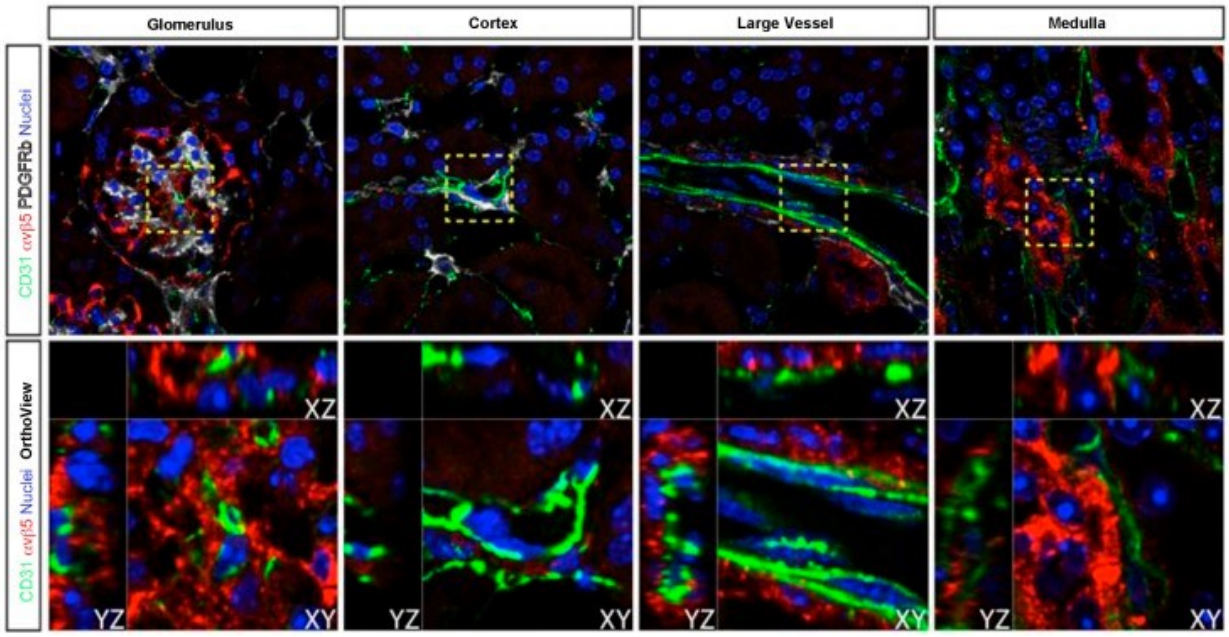

Characterization of *αvβ5* integrin expression in the kidney. Frozen sections of mouse kidney were stained for *αvβ5* (red), CD31 (green), and PDGFR*β* (white) with nuclei in blue. Representative images (63× magnification) from the glomerulus, cortex, medulla as well as an artery are shown. *αvβ5* is expressed in podocytes, mesangial, epithelial, and perivascular cells of the kidney and within interstitial cells, and appears to be present within PDGFR*β*-positive cells, but not in CD31-positive endothelial cells.

Figure 7.

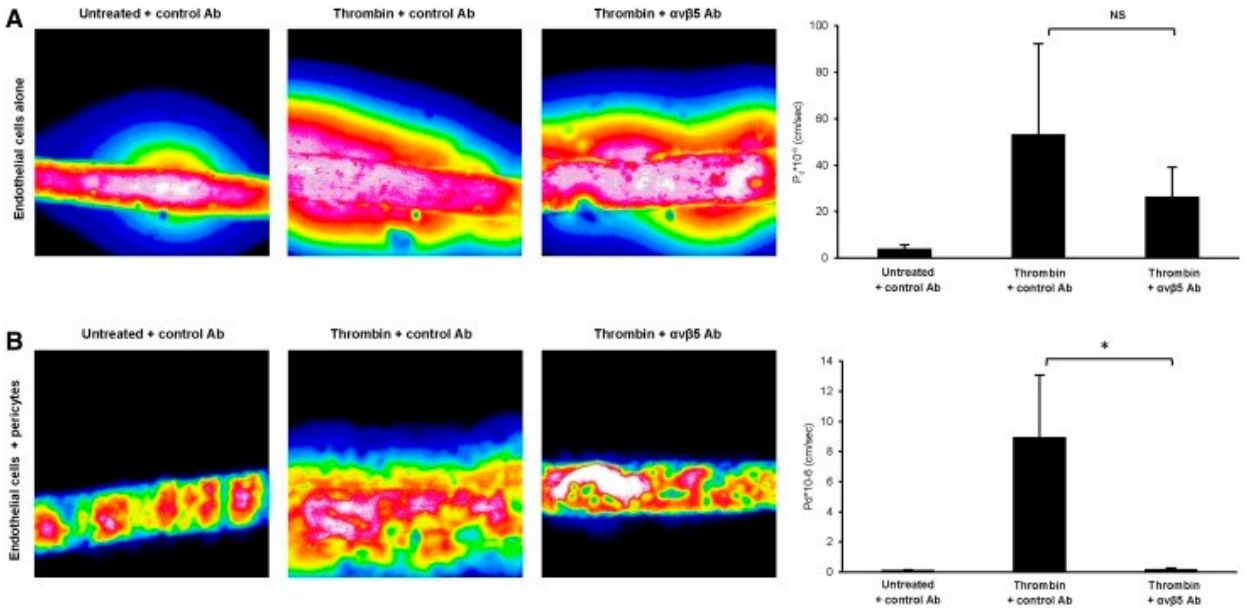

αvβ5 regulates vascular permeability in a pericyte-dependent manner. (A) Human kidney endothelial cells were seeded into a three-dimensional microfluidic device and allowed to form a tube in the presence of flow. Cells were treated with control or *αvβ5* antibody 1 hour before challenge with thrombin (3 U/ml). 70 kD Texas Red albumin was perfused into the vessel and the diffusion was measured by confocal microscopy to calculate the diffusive permeability coefficient (P_d). No significant difference was observed with *αvβ5* antibody with endothelial cells alone (n=6). (B) All conditions are the same as described above except human kidney pericytes are first seeded into the microfluidics device, followed by seeding with the endothelial cells. In this condition, the *αvβ5* antibody significantly inhibited the thrombin-induced vascular permeability. *P<0.05 versus thrombin + control antibody; error bars = SEM.

Figure 8.

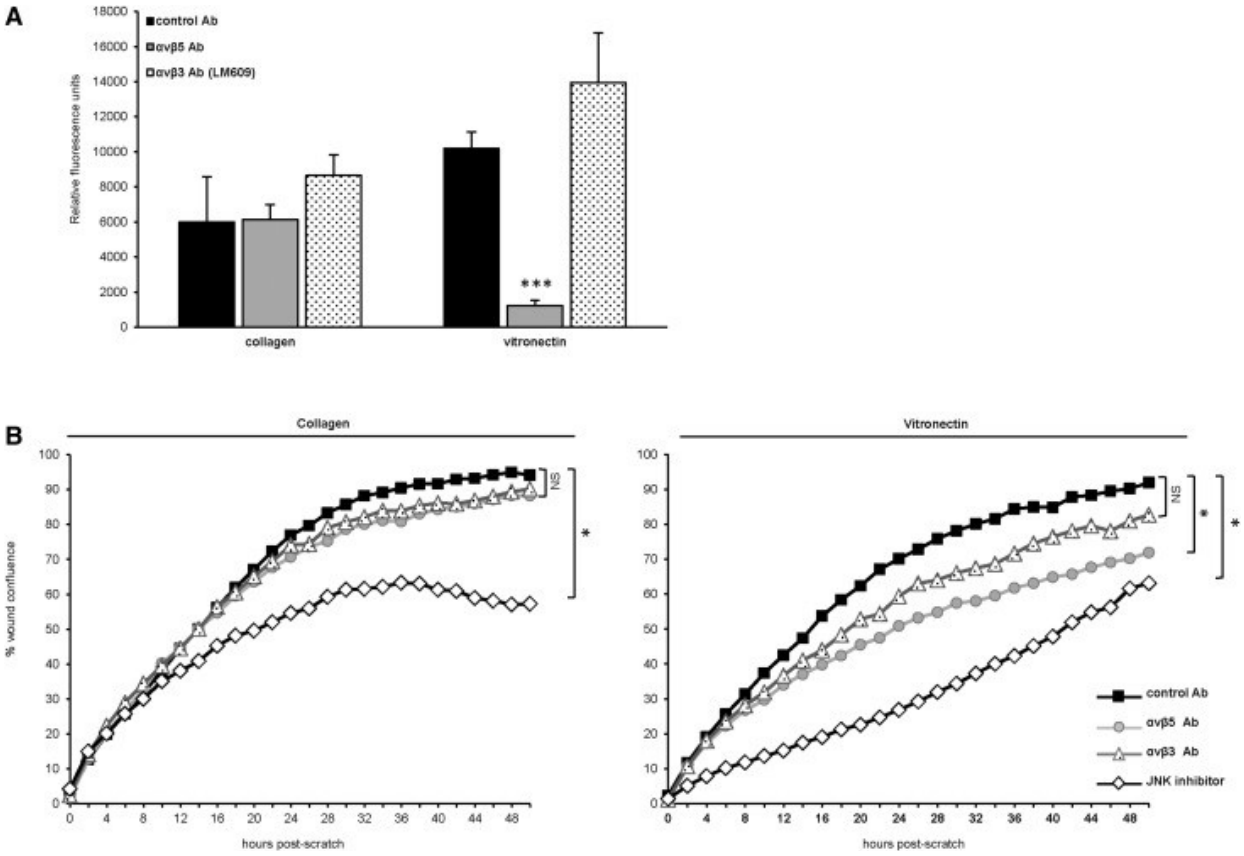

αvβ5 regulates pericyte adhesion and migration on vitronectin. Human kidney pericytes were seeded on plates coated with collagen or vitronectin. (A) Fluorescently labeled cells are seeded in the presence of the *αvβ5* antibody, an *αvβ3* antibody, or a control antibody and were counted after washing the adherent cells. The *αvβ5* antibody significantly reduced adhesion of cells on vitronectin compared with control antibody treatment. ****P*<0.001 versus control antibody; error bars = SEM. (B) Cells were treated with antibody 1 hour before scratch wound, and images were taken every 2 hours for 2 days and wound confluence was calculated. The *αvβ3* antibody had no significant effect on migration, the JNK inhibitor SP600125 (included as a positive control) inhibited migration on both substrates and the *αvβ5* antibody significantly inhibited migration of pericytes on vitronectin. **P*<0.05 versus control antibody.

Figure 9.

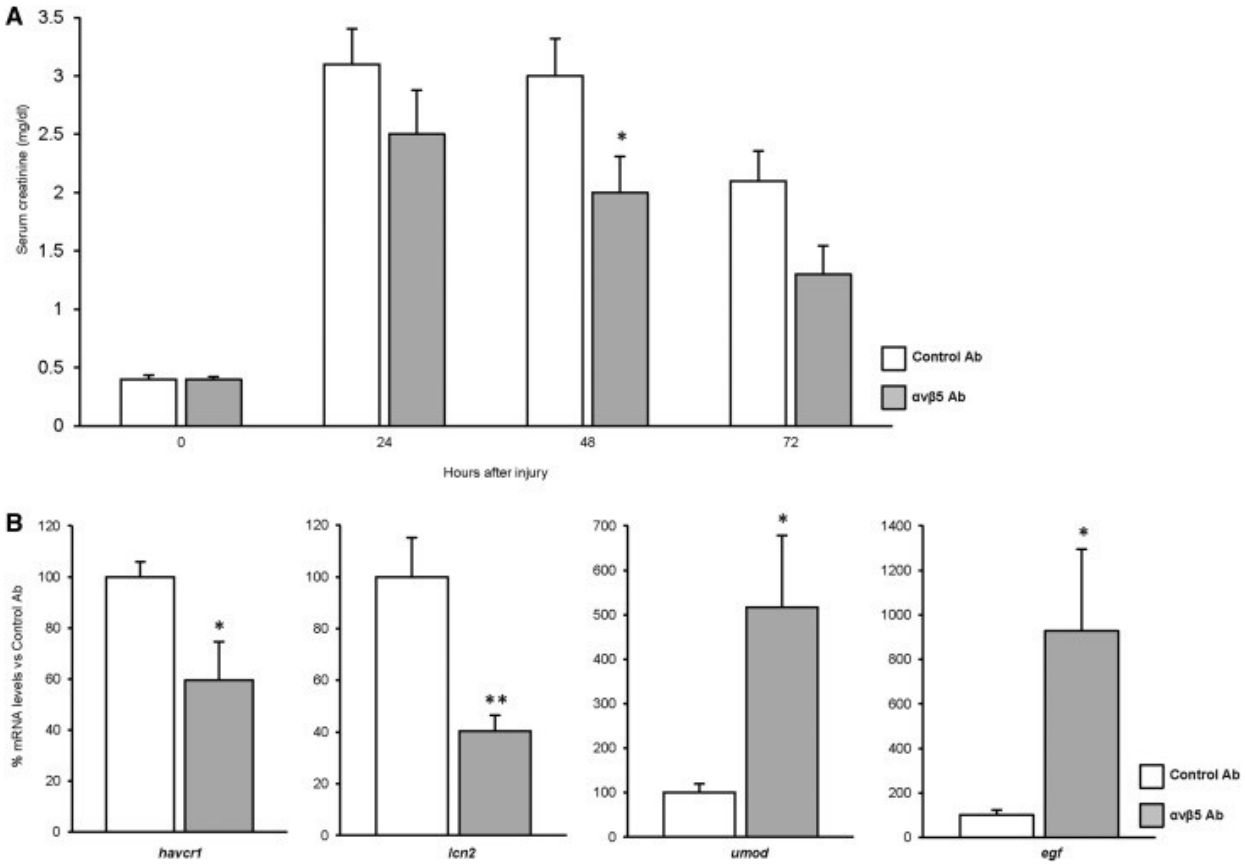

Treatment with *αvβ5* antibody after ischemia provides protection from injury. (A) Rats were treated with a single dose (3 mg/kg) of *αvβ5* antibody 8 hours postclamp release. This single dose was effective in attenuating ischemia-induced serum creatinine increases at 48 hours postinjury. **P*<0.05 versus control antibody; error bars = SEM. **(**B**)** Kidneys were harvested at 72 hours postclamp from the study in A for quantitative PCR analysis. At 8 hours postclamp, treatment significantly reduced the expression of two biomarkers induced by injury (*havcr1*, *lcn2*) and increased the expression of two biomarkers diminished by injury (*umod*, *egf*). **P*<0.05; ***P*<0.01 versus control antibody; error bars = SEM.